European Radiology (2020) 30:1866–1875
https://doi.org/10.1007/s00330-019-06536-7

MAGNETIC RESONANCE

Increased diagnostic accuracy of giant cell arteritis using three-dimensional fat-saturated contrast-enhanced vessel-wall magnetic resonance imaging at 3 T

Guillaume Poillon[1,2] · Adrien Collin[1] · Ygal Benhamou[3] · Gaëlle Clavel[4] · Julien Savatovsky[1] · Cécile Pinson[2] · Kevin Zuber[5] · Frédérique Charbonneau[1] · Catherine Vignal[6] · Hervé Picard[4,5] · Tifenn Leturcq[4] · Sébastien Miranda[3] · Thomas Sené[4] · Emmanuel Gerardin[2] · Augustin Lecler[1]

Received: 18 June 2019 / Revised: 8 October 2019 / Accepted: 22 October 2019 / Published online: 6 December 2019

Abstract

Objectives To compare the diagnostic accuracy of 3D versus 2D contrast-enhanced vessel-wall (CE-VW) MRI of extracranial and intracranial arteries in the diagnosis of GCA.

Methods This prospective two-center study was approved by a national research ethics board and enrolled participants from December 2014 to October 2017. A protocol including both a 2D and a 3D CE-VW MRI at 3 T was performed in all patients. Two neuroradiologists, blinded to clinical data, individually analyzed separately and in random order 2D and 3D sequences in the axial plane only or with reformatting. The primary judgment criterion was the presence of GCA-related inflammatory changes of extracranial arteries. Secondary judgment criteria included inflammatory changes of intracranial arteries and the presence of artifacts. A McNemar's test was used to compare 2D to 3D CE-VW MRIs.

Results Seventy-nine participants were included in the study (42 men and 37 women, mean age 75 (± 9.5 years)). Fifty-one had a final diagnosis of GCA. Reformatted 3D CE-VW was significantly more sensitive than axial-only 3D CE-VW or 2D CE-VW when showing inflammatory change of extracranial arteries: 41/51(80%) versus 37/51 (73%) (p = 0.046) and 35/50 (70%) (p = 0.03). Reformatted 3D CE-VW was significantly more specific than 2D CE-VW: 27/27 (100%) versus 22/26 (85%) (p = 0.04). 3D CE-VW showed higher sensitivity than 2D CE-VW when detecting inflammatory changes of intracranial arteries: 10/51(20%) versus 4/50(8%), p = 0.01. Interobserver agreement was excellent for both 2D and 3D CE-VW MRI: κ = 0.84 and 0.82 respectively.

Conclusions 3D CE-VW MRI supported more accurate diagnoses of GCA than 2D CE-VW.

Key Points

- *3D contrast-enhanced vessel-wall magnetic resonance imaging is a high accuracy, non-invasive diagnostic tool used to diagnose giant cell arteritis.*
- *3D contrast-enhanced vessel-wall imaging is feasible for clinicians to complete within a relatively short time, allowing immediate assessment of extra and intracranial arteries.*
- *3D contrast-enhanced vessel-wall magnetic resonance imaging might be considered a diagnostic tool when intracranial manifestation of GCA is suspected.*

Keywords Magnetic resonance imaging · Giant cell arteritis · Diagnosis · Two-dimensional · Three-dimensional

✉ Augustin Lecler
alecler@for.paris

[1] Department of Neuroradiology, Foundation Adolphe de Rothschild Hospital, 29 rue Manin, 75019 Paris, France

[2] Department of Neuroradiology, Rouen University Hospital, Rouen, France

[3] Department of Internal Medicine, Rouen University Hospital, Normandie Univ, UNIROUEN, INSERM U1096, Rouen, France

[4] Department of Internal Medicine, Foundation Adolphe de Rothschild Hospital, Paris, France

[5] Department of Clinical Research, Foundation Adolphe de Rothschild Hospital, Paris, France

[6] Department of Ophthalmology, Foundation Adolphe de Rothschild Hospital, Paris, France

Abbreviations

2D	Two-dimensional
3D CE-VW	Three-dimensional fat-saturated contrast-enhanced vessel-wall
ASNR	American Society of Neuroradiology
CE-VW	Contrast-enhanced vessel-wall
CRP	C-reactive protein
ESR	Erythrocyte sedimentation rate
EULAR	European League Against Rheumatism
GCA	Giant cell arteritis
MR	Magnetic resonance
MRI	Magnetic resonance imaging
NPV	Negative predictive values
PPV	Positive predictive values
ROC	Receiver operating characteristic
SPAIR	Spectral Attenuated Inversion Recovery
STARD	Standards for Reporting of Diagnostic Accuracy
TAB	Temporal artery biopsy
WI	Weighted-imaging

Introduction

Giant cell arteritis (GCA) is the most common chronic inflammatory vasculitis of large- and medium-sized arteries [1, 2]. Its origin remains poorly understood [3, 4]. Its typical histological features consist of a polymorphic granulomatous infiltrate affecting the three tunics of the arterial wall, more specifically the inner part of the media in a segmented and multifocal distribution [5, 6]. Accurate diagnosis is urgent due to potential serious ophthalmological and systemic complications [7].

Temporal artery biopsy (TAB) remains the reference for diagnosing GCA, but has been challenged by imaging of extracranial and intracranial arteries with high-resolution magnetic resonance (MR), which has proven to be highly sensitive when diagnosing GCA [8–14]. Recently, the European League Against Rheumatism (EULAR) mentioned MRI as an adequate tool to help clinicians diagnose GCA [15]. However, the volume explored by optimized two-dimensional (2D) contrast-enhanced vessel-wall (CE-VW) MR sequences developed for imaging extracranial arteries is limited, failing to cover the entire course of the arteries. In addition, some arterial segments have an anatomical arrangement parallel to the transverse plane, causing partial volume effects that make it difficult to evaluate precisely wall thickening and mural enhancement [8–14].

Three-dimensional fat-saturated contrast-enhanced vessel-wall (3D CE-VW) MRI might be useful to overcome these issues within a time frame compatible with clinical practice. Moreover, 3D sequences might allow simultaneous analysis of intracranial and extracranial arteries.

The objective of our study was to compare diagnostic accuracy when using 3D versus 2D CE-VW MRI when diagnosing GCA.

Materials and methods

Ethics committee approval

This prospective multicenter study was conducted in two tertiary referral centers. It was approved by two independent research ethics boards (ID RCB 2016-A01043-48 and ID RCB 2019-3, NCT 02896647). It adhered to the tenants of the Declaration of Helsinki. Signed informed consent was obtained from all subjects. This study follows the Standards for Reporting of Diagnostic Accuracy Studies (STARD) guidelines [16].

Population

From December 2014 to October 2017, 79 participants were included. Inclusion criteria were as follows: (a) patients aged 50 years or older; (b) suspicion of GCA based on the presence of the following criteria: constitutional symptoms (anorexia, weight loss, fever, asthenia, malaise), new onset headache or neck pain, induration or pain of the temporal artery, jaw claudication, tongue or swallowing disorders, polymyalgia rheumatica, ophthalmological findings (transient visual loss or diplopia, unilateral or bilateral visual loss from anterior ischemic optic neuropathy or occlusion of the central retinal artery, diplopia secondary to ocular motor palsy or extraocular muscle ischemia), abnormal laboratory results (erythrocyte sedimentation rate (ESR), C-reactive protein (CRP) level); (c) completion of an MRI with CE-VW sequences.

Patients with any contraindications to MRI, patients with known GCA, or patients with a TAB prior to MRI were not included. The exclusion criterion was the absence of both 2D and 3D CE-VW sequences. Selection of patients is shown in Fig. 1. Among the 79 patients included, four CE-VW sequences were missing for analysis: one 2D CE-VW and one 3D CE-VW due to major artifacts preventing MR analysis and two incomplete 2D CE-VW due to a patient's discomforting leading to premature interruption of the MRI protocol.

Clinical and biological data

Systemic symptoms (anorexia, weight loss, fever, asthenia, jaw claudication, headache, scalp tenderness, induration or pain of the temporal artery, neck pain, myalgia, malaise, tongue or swallowing disorders) and other ophthalmological findings (transient visual symptoms, visual acuity, diplopia, ocular motor examination, appearance of the ocular fundus) were noted at admission. Urgent laboratory testing included

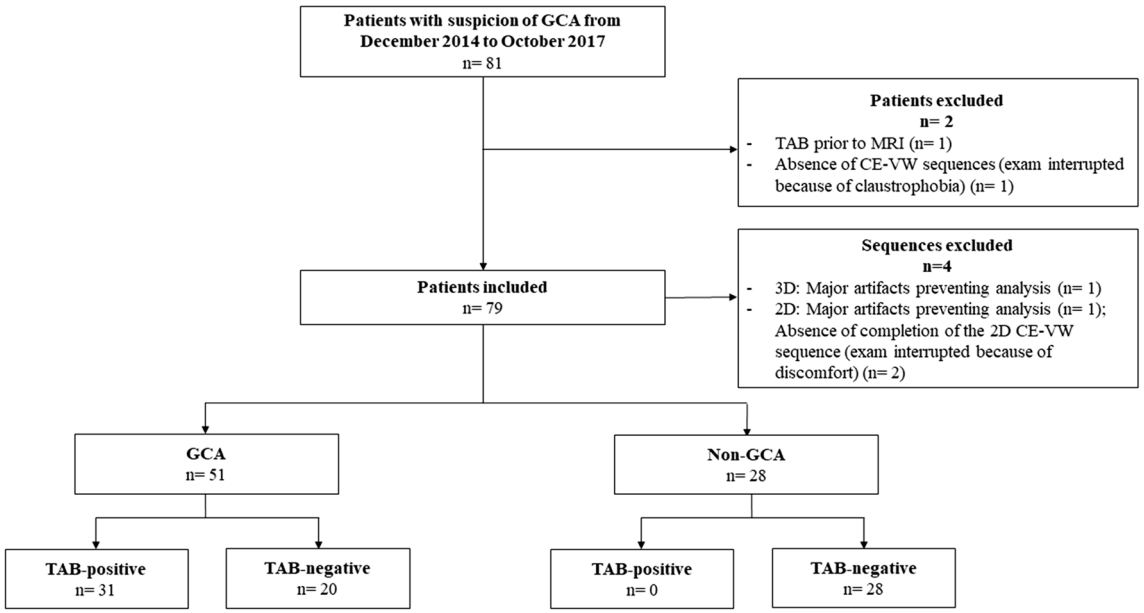

Fig. 1 Flow chart showing selection of patients. GCA: giant-cell arteritis; TAB: temporal artery biopsy; CE-VW: contrast-enhanced vessel-wall

tests for an inflammatory biologic syndrome (ESR, CRP, complete blood count, platelet count). A TAB was performed to assess the presence of GCA.

Diagnostic reference

A final diagnosis of GCA was made in the case of a positive TAB. In patients with a negative TAB, a review of the clinical and biological charts including response to corticosteroid therapy (but excluding MRI findings) was performed by an interdisciplinary panel of rheumatologists and internists not involved in the management of the patient. By consensus, they established a final diagnosis of GCA based on ACR criteria [17].

MR imaging

MR imaging was performed on a 3 T Philips Ingenia (Philips Medical Systems) or a 3 T General Electric Discovery MR 750 (General Electric Medical Systems) with a dedicated 32-channel head coil. Based on the American Society of Neuroradiology (ASNR) vessel wall imaging guidelines [18], proton density-weighted fat-saturated 2D and 3D CE-VW sequences were acquired before and after injection of a single intravenous bolus (0.1 mmol/kg) of gadobutrol (Gadovist®, Bayer Healthcare). A Spectral Attenuated Inversion Recovery (SPAIR) on the 3 T Philips Ingenia and a spectral presaturation (FatSat) on the 3 T GE Discovery MR750 were used for fat suppression to offer the best contrast between extracranial vessels wall inflammation and the surrounding fat.

To avoid any effect due to impregnation, sequences were performed in a random order. Characteristics of CE-VW MR sequences are displayed in Table 1.

MRI analysis

Two board-certified neuroradiologists (AC and GP), with 5 and 2 years of experience, respectively, blinded to clinical, biological, and histopathologic data, independently read the randomized results of the anonymized 2D and 3D CE-VW MRI sequences. A second reading was performed 8 weeks later to analyze intra-observer concordance. Six weeks later, a "gold standard" consensus reading was performed with a third reader, a second senior neuroradiologist with 9 years of experience (AL), who was also blinded to the data. Subsequently, a more detailed analysis of the 3D CE-VW sequence was performed to more precisely evaluate the effect of the multiplanar reformatting. The same readers interpreted the randomized results of the 3D CE-VW MRI sequences in the axial plane only or with multiplanar reformatting. All reading sessions took place on a dedicated workstation with the Horos software (Horosproject.org, Nimble Co).

The readers assessed the following characteristics of patients' MRIs:

– The primary judgment criterion was the presence of GCA-related inflammatory changes of extracranial arteries, based on the search for circumferential wall thickening and mural enhancement of the six following extra-cranial arterial segments: left and right frontal and parietal branches of the superficial temporal artery and of the occipital artery, using the previously published 4-point scale [8, 12].

Table 1 Detailed characteristics of CE-VW MR sequences. CE-VW: contrast-enhanced vessel-wall; PD: proton density; TR: repetition time; TE: echo time; FOV: field of view; SPAIR: spectral attenuated inversion recovery; FatSat: spectral presaturation

	Center 1 (n = 45)		Center 2 (n = 34)	
	3-T Philips Ingenia		3-T General Electric Discovery MR 750	
	2D CE-VW	3D CE-VW	2D CE-VW	3D CE-VW
Scan mode	2D	3D	2D	3D
Type of sequence	PD-weighted	PD-weighted	PD-weighted	PD-weighted
TR (ms)	1350	550	500	600
TE (ms)	30	38	22	30
Number of excitations	1	2	4	2
FOV (mm)	220 × 220	252 × 252 × 200	200 × 200	200 × 200 × 177
Bandwidth (kHz)	528	754	31.3	62.5
Acquisition matrix	736 × 736	316 × 316 × 250	512 × 416	288 × 288 × 148
Acquired voxel size (mm)	0.3 × 0.3 × 1.5	0.8 × 0.8 × 0.8	0.4 × 0.5 × 3	0.7 × 0.7 × 1.2
Reconstructed voxel size (mm)	0.3 × 0.3 × 1.5	0.8 × 0.8 × 0.8	0.4 × 0.5 × 3	0.7 × 0.7 × 0.6
Acquisition duration	4 min 20 s	4 min 51 s	5 min 19 s	6 min 50 s
Fat saturation	SPAIR	SPAIR	FatSat	FatSat

- Score 0: no wall thickening (< 0.6 mm) and no mural enhancement
- Score 1: no wall thickening (< 0.6 mm) and slight mural enhancement
- Score 2: wall thickening (> 0.6 mm) and substantial mural enhancement
- Score 3: marked wall thickening (> 0.7 mm) and strong mural enhancement with perivascular inflammatory infiltration

Scores 0 and 1 were considered negative for GCA, whereas scores 2 and 3 were considered positive. At least one positive segment out of the six analyzed was required to establish a positive MRI diagnosis of GCA. Examples are provided in Fig. 2.

- Secondary judgment criteria were:
- The presence of GCA-related inflammatory changes of the following intracranial arteries: the internal carotid artery after its exit from the cavernous sinus; the vertebral artery at least 0.5 cm from its emergence from the transverse canal of the first cervical vertebrae; the anterior, middle, and posterior cerebral arteries; the basilar artery. The evaluation of their wall thickening and mural enhancement used the following 4-point scale:

- Score 0: no wall thickening and no mural enhancement
- Score 1: no wall thickening and slight mural enhancement
- Score 2: wall thickening and substantial mural enhancement
- Score 3: marked wall thickening and strong mural enhancement with perivascular inflammatory infiltration

Scores 0 and 1 were considered negative for GCA-related inflammatory changes, whereas scores 2 and 3 were considered positive for GCA-related inflammatory changes. At least one positive segment was required to establish a positive MRI diagnosis of GCA-related inflammatory changes of the intracranial arteries.

- The presence of artifacts scored as follows: 0 corresponding to an absence of artifacts, 1 corresponding to the presence of minor artifacts not preventing the MR analysis, 2 to the presence of major artifacts not preventing MR analysis, 3 to the presence of major artifacts preventing MR analysis.

Statistical analysis

Quantitative variables were presented as mean (standard deviation), median (interquartile range or IQR), and categorical variables as percentages. Accuracy, sensitivity, specificity, positive predictive values (PPVs), and negative predictive values (NPVs) were calculated for each CE-VW MR sequence. Diagnostic accuracy was compared using the McNemar test. Inter- and intra-observer agreement for MRI reading was assessed using non-weighted Cohen's kappa statistics and interpreted as follows: 0.0–0.2—poor correlation; 0.21–0.4—fair correlation; 0.41–0.6—moderate correlation; 0.61–0.8—good correlation; 0.81–1—almost perfect correlation [19]. The influence of a delay between introducing corticosteroids and completion of the MRI was studied by using receiver operating characteristic (ROC) curves. Optimal thresholds were calculated from ROC curves using the

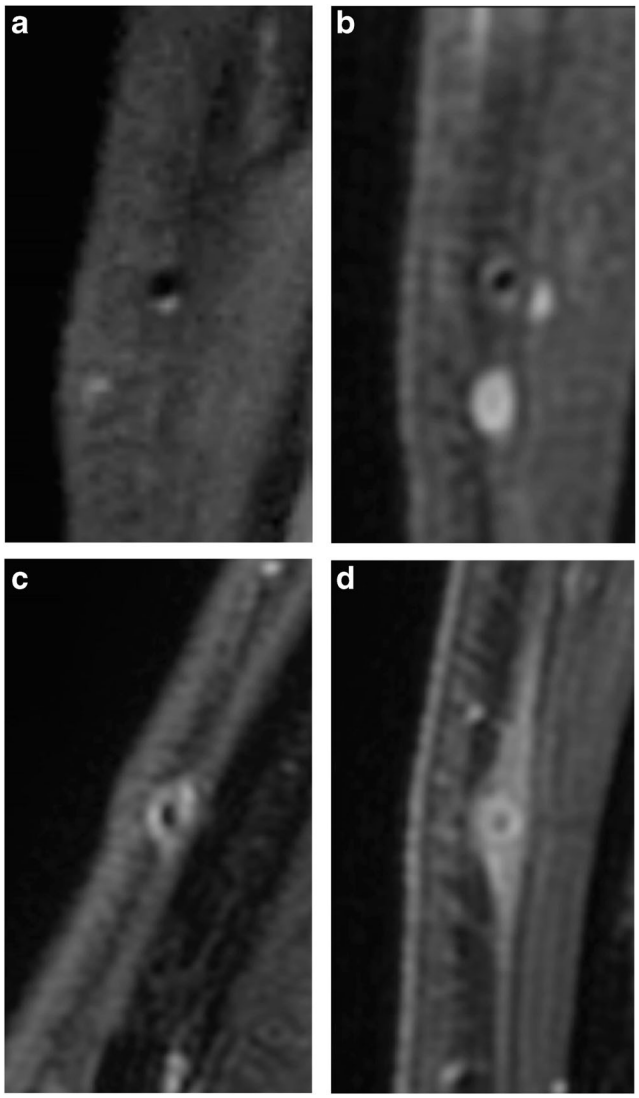

Fig. 2 Contrast-enhanced fat saturation proton density-weighted MRI at 3 T of 4 different patients illustrating typical images of the 4-point scale used to assess the extracranial arteries. **a** No wall thickening (< 0.6 mm) and no mural enhancement, rating 0. **b** No wall thickening (< 0.6 mm) and slight mural enhancement, rating 1. **c** Wall thickening (> 0.6 mm) and substantial mural enhancement, rating 2. **d** Marked wall thickening (> 0.7 mm) and strong mural enhancement with perivascular inflammatory infiltration, rating 3

Youden index. A p value below 0.05 was considered statistically significant. Data were analyzed using the R software package [20].

Results

Demographic, clinical, and biological characteristics

Seventy-nine participants were included in the study (42 men and 37 women, mean age 75 years [SD 9.5]). Fifty-one had a final diagnosis of GCA (26 women and 25 men). There were no differences between the two groups for the clinical and biological characteristics, except for initial ESR and C-reactive protein rates, which were significantly higher in GCA patients. Detailed characteristics are displayed in Table 2.

TAB diagnostic accuracy

TAB was positive for 31 patients. Its sensitivity, specificity, PPV, and NPV were 62%, 100%, 100%, and 58% respectively (Table 3).

GCA-related inflammatory changes of extracranial arteries

Reformatted 3D CE-VW was significantly more sensitive than axial-only 3D CE-VW or 2D CE-VW when showing inflammatory change of extracranial arteries: 41/51 (80%) versus 37/51 (73%) ($p = 0.046$) and 35/50 (70%) ($p = 0.03$). Reformatted 3D CE-VW was significantly more specific than 2D CE-VW: 27/27 (100%) versus 22/26 (85%) ($p = 0.04$).

There was no significant difference in sensitivity and specificity between axial-only 3D CE-VW and 2D CE-VW: 37/51 (73%) versus 35/50 (70%) ($p = 0.32$) and 25/27 (93%) versus 22/26 (85%) ($p = 0.16$), respectively (Table 3 and Figs. 3 and 4).

GCA-related inflammatory changes of intracranial arteries

3D CE-VW sequences were significantly more sensitive than 2D CE-VW when showing GCA-related inflammatory changes: 10/51 (20%) versus 4/50 (8%) patients ($p = 0.01$) (Table 3 and Fig. 5). Bilateral intracranial involvement was detected in 7 (70%) patients versus 1 (25%) with 3D and 2D CE-VW respectively. Inflammatory changes of any internal carotid arteries, any vertebral arteries, or any arteries of the Circle of Willis were detected in 8/10 (80%), 9/10 (90%), and 2/10

Table 2 Clinical and biological characteristics of GCA and non-GCA patients. The results in brackets are percentages. The asterisks (*) indicate significant differences after appropriate statistical correction. GCA: giant-cell arteritis; IQR: interquartile range; ESR: erythrocyte sedimentation rate; CRP: C-reactive protein

		GCA $n = 51$	Non-GCA $n = 28$	p
Gender	Men Women	25 (49) 26 (51)	17 (60.7) 11 (39.3)	0.4
Age	Median [IQR]	77 [12.5]	71 [12]	0.1
ESR	Median [IQR]	71 [55.5]	41 [63]	0.005*
CRP	Median [IQR]	72.5 [78.6]	17 [31]	< 0.0001*

Table 3 Diagnostic accuracy and inter and intra-reader agreement of 2D and 3D contrast-enhanced vessel-wall (CE-VW) MRI and of temporal artery biopsy (TAB) for distinguishing giant-cell arteritis (GCA) from non-GCA patients. An asterisk (*) indicates a statistically significant difference. *PPV*: positive predictive value; *NPV*: negative predictive value; *IQR*: interquartile ratio; *NA*: not applicable, *NS*: not significant

	Inflammatory changes of extracranial arteries						Inflammatory changes of intracranial arteries			TAB
	2D CE-VW	Axial-only 3D CE-VW	Reformatted 3D CE-VW	2D CE-VW versus axial-only 3D CE-VW	2D CE-VW versus reformatted 3D CE-VW	Axial-only 3D CE-VW versus reformatted 3D CE-VW	2D CE-VW	3D CE-VW	2D CE-VW versus 3D CE-VW	
Accuracy	0.75	0.79	0.87				0.48	0.40		0.75
Sensitivity	70%	73%	80%	$p = 0.32$	$p = 0.03$*	$p = 0.046$*	8%	20%	$p = 0.01$*	62%
Specificity	85%	93%	100%	$p = 0.16$	$p = 0.04$*	$p = 0.16$	100%	100%	NA	100%
PPV	90%	95%	100%	$p = 0.14$	$p = 0.04$*	$p = 0.15$	100%	100%	NA	100%
NPV	59%	64%	73%	$p = 0.09$	$p = 0.004$*	$p = 0.017$*	37%	41%	$p = 0.02$*	58%
Inter-reader agreement	0.84	0.92	0.82				0.49	0.72		
Intra-reader agreement	0.81	0.90	1				0.71	0.96		

(20%) patients versus 1/4 (25%), 4/4 (100%), and 0/4 (0%) patients with 3D and 2D CE-VW respectively.

Presence of artifacts

There were no significant differences when scoring artifacts between 2D and 3D sequences with a median score of 0.5 (IQR 0.7) and 0.4 (IQR 0.6), $p = 0.6$, respectively.

Inter-and intra-reader agreement

Regarding assessment of GCA-related inflammatory changes of extracranial arteries, inter- and intra-observer agreements were almost perfect, with a Cohen's κ of 0.84 (IC95 0.66–0.95) and 0.81 (IC95 0.40–1) for 2D CE-VW, 0.92 (IC95 0.80–0.97) and 0.90 (IC95 0.77–0.97) for axial-only 3D CE-VW, and 0.82 (IC95 0.66–0.92) and 1 (IC95 0.82–1) for reformatted 3D CE-VW, respectively.

Regarding assessment of GCA-related inflammatory changes of intracranial arteries, the inter-observer agreement was moderate for 2D and good for 3D sequences, with a Cohen's κ of 0.49 (0.16–0.82) and 0.72 (IC95 0.46–0.90) respectively. Intra-observer agreement was good for 2D sequences and almost perfect for 3D sequences, with a Cohen's κ of 0.71 (IC95 0.27–1) and 0.96 (0.75–1) respectively.

Impact of the delay between the completion of the MRI and corticosteroid therapy

Patients with an accurate diagnosis of GCA with 2D and 3D CE-VW MRI had a shorter corticosteroid-MRI interval than patients with an inaccurate diagnosis: 1 day versus 3 days ($p = 0.048$) and 2 days versus 4 days ($p = 0.052$) respectively. ROC curves provided optimal thresholds for accurate diagnosis of GCA within the first 3 days and 5 days after starting corticosteroid therapy for 2D CE-VW and 3D CE-VW respectively.

Discussion

Our prospective study showed that 3D CE-VW MRI had a higher accuracy than 2D CE-VW when diagnosing GCA, with 80% sensitivity and 100% specificity.

Our results are in line with previous studies evaluating diagnostic accuracy of extracranial arteries MRI in GCA, with a sensitivity of our 2D CE-VW sequence of 70% and a specificity of 85% similar to the 69% to 81% sensitivity and 80 to 97% specificity reported in the literature [8, 12–14]. While excellent sensitivity and specificity values of 3D CE-VW MRI sequences have been demonstrated for the diagnosis of arteritic anterior ischemic optic neuropathy in patients with GCA [21, 22], our study is the first one to our knowledge to provide diagnostic accuracy of a 3D CE-VW MRI sequence for GCA.

We showed that multiplanar reformatted 3D CE-VW imaging was more sensitive and specific when diagnosing GCA as compared to axial-only 3D CE-VW and 2D CE-VW. This suggests that reformatting 3D images without significant loss to image resolution might be the main factor accounting for higher diagnostic accuracy. 3D CE-VW is particularly interesting when diagnosing GCA because it allows reformatting MR images in an oblique sagittal plane to align and analyze branches of extracranial arteries along their whole course,

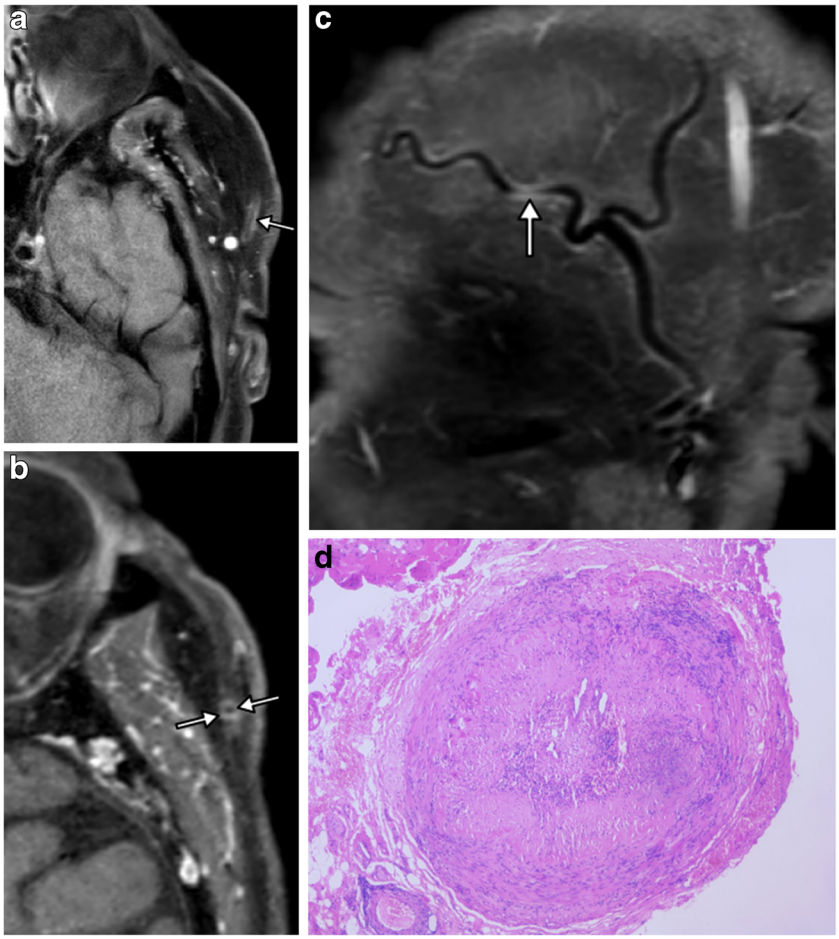

Fig. 3 Contrast-enhanced vessel-wall (CE-VW) MRI in an 82-year-old man with suspicion of giant-cell arteritis (GCA). Extracranial arteries were considered negative for GCA on 2D CE-VW MRI and positive on 3D CE-VW-MRI. The discrepancy centered around the evaluation of the anterior branch of the left temporal artery. On native axial 2D CE-VW (**a**), readers found that the slight mural enhancement was not circumferential (arrow), therefore did not consider it positive for GCA. On 3D CE-VW MRI reformatted in a para-axial perpendicular plane to the course of the artery (**b**), the arterial wall enhancement appeared more clearly and circumferential (arrows), therefore deemed positive for GCA. 3D CE-VW MRI reformatted in a sagittal oblique plane (**c**) showed very short focal inflammatory changes of a horizontal segment of the artery (arrow), explaining the difficulties to assess it accurately on axial 2D CE-VW. All other extracranial artery segments were considered normal on both 2D and 3D CE-VW imaging. Temporal artery biopsy (**d**) confirmed GCA

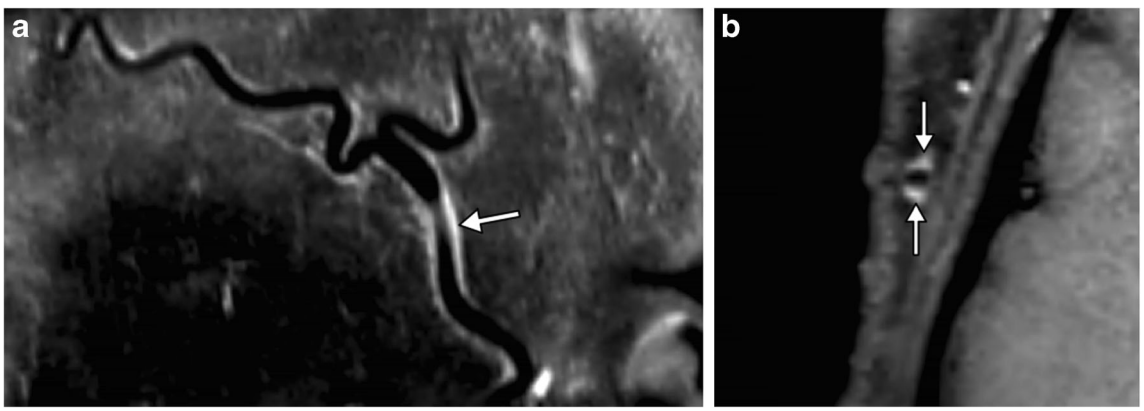

Fig. 4 Contrast-enhanced vessel-wall (CE-VW) MRI in a 70-year-old woman with suspicion of giant-cell arteritis (GCA). 3D CE-VW MRI reformatted in a sagittal plane (**a**) showing a focal area of enhancement surrounding the right temporal artery (arrow) compatible with GCA-related inflammatory changes. 3D CE-VW MRI reformatted in a para-axial perpendicular plane to this area (**b**) showing that the enhancement was not circumferential (arrows), corresponding to venous plexuses adjacent to the artery. Using 3D CE-VW supported quick and reliable identification of such pitfalls by allowing multiplanar reconstructions. Temporal artery biopsy was negative for GCA and final consensus evaluation ruled out GCA

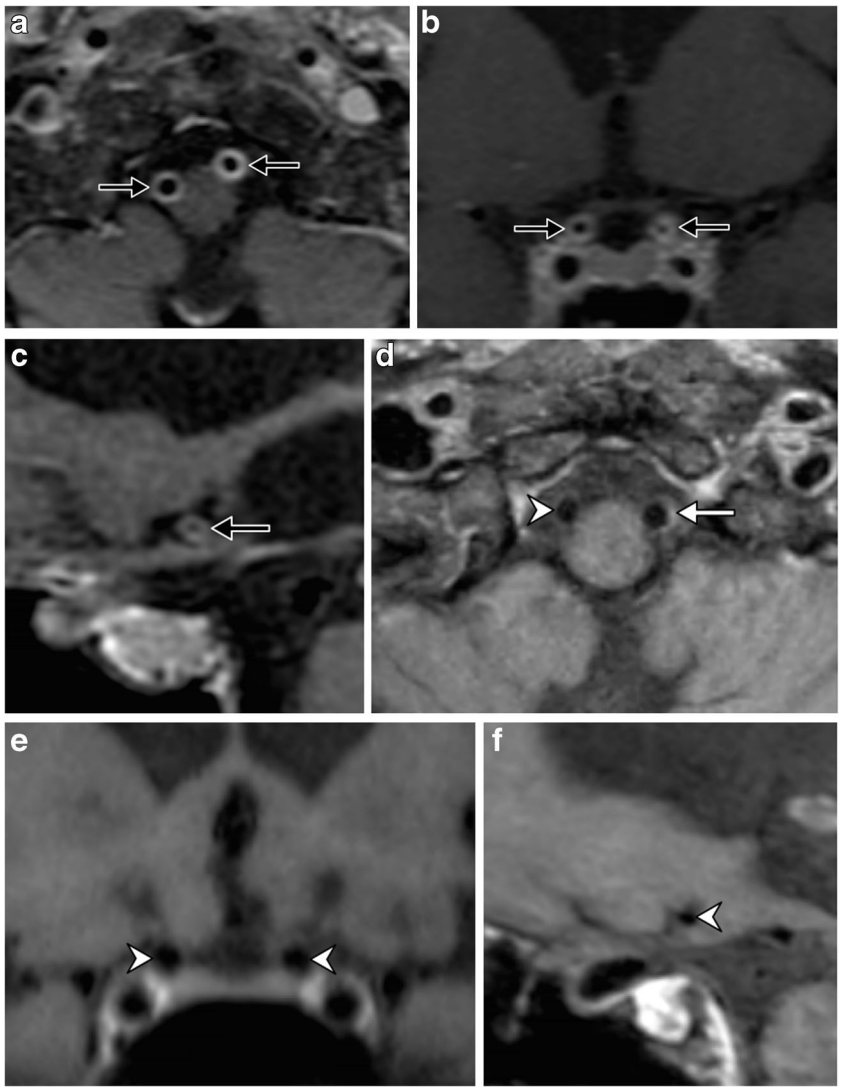

Fig. 5 Contrast-enhanced vessel-wall (CE-VW) MRI in a 75-year-old man with histopathologically confirmed giant-cell arteritis (GCA). 3D CE-VW MRI reformatted in axial (**a**), coronal (**b**), and sagittal (**c**) planes showing clear circumferential enhancement and thickening (black arrows) of both V4 segments of vertebral arteries, both internal carotid arteries after exiting from the cavernous sinus and left middle cerebral artery. In comparison, 3D CE-VW MRI reformatted in axial (**d**), coronal (**e**), and sagittal (**f**) planes in a 73-year-old woman ruled out GCA, showing a normal-appearing right vertebral artery, internal carotid arteries and middle cerebral artery (arrowhead) and mild eccentric enhancement of the V4 segment of the left vertebral artery (white arrow), ultimately not considered GCA-related inflammatory changes, but rather atherosclerosis

displaying wall thickening and mural enhancement more conspicuously, thus revealing GCA-inflammatory changes more easily. Subsequently, 3D CE-VW reformatting in a strictly perpendicular orientation to the arteries supports higher diagnostic confidence when confirming GCA by showing circumferential arterial changes. Using 3D CE-VW might decrease the rate of false negative such as in cases of distal or focal inflammatory changes, which might be difficult to assess with 2D CE-VW, or in cases where arterial segments cannot be correctly appreciated because of their tangential orientation to the transversal plane [8, 23]. This is crucial in GCA because the disease can be segmented and multifocal [24]. 3D CE-VW might reduce the rate of false positive findings due to small venous plexuses adjacent to the artery or of atheromatous plaques, which do not involve the whole circumference of the artery [25].

3D CE-VW sequences were also significantly more sensitive than 2D CE-VW when showing GCA-related inflammatory changes of intracranial arteries. We found involvement of intracranial arteries in 20% of our GCA patients, which supports findings from previous studies [14, 26–28]. 3D CE-VW may support easier diagnosis of GCA-related intracranial inflammation and help distinguish GCA from atherosclerosis, which has a high prevalence in older patients and is the main differential diagnosis. Indeed, 3D CE-VW MRI differentiates between concentric wall thickening, suggestive of vasculitis, and eccentric wall thickening, more commonly found in atherosclerosis. This distinction might be challenging to perform with 2D CE-VW, whereas the possibility of reformatting enables 3D CE-VW to overcome major issues such as partial volume effect [18, 29].

3D CE-VW sequences can be provided with an acceptable duration (4 min 51 s to 6 min 50 s in our study) for clinical practice. This is particularly important in patients with a suspicion of GCA because of the morbidity related to the disease requiring emergency treatment and therefore a quick diagnosis [30]. 3D CE-VW suffered only minor artifacts, with a similarly low score of artifacts when compared to 2D CE-VW imaging. Moreover, inter- and intra-reader agreements were almost perfect

with 3D CE-VW MRI, meaning that diagnosing GCA with 3D CE-VW MRI might be feasible in clinical practice without involving radiologists with further sub-specialized training.

In the case of suspicion of GCA, the relevance of TAB in the diagnostic strategy is discussed [31–33]. In our study, 3D CE-VW MRI had a significantly higher sensitivity than TAB. TAB is an invasive procedure and its results are delayed. These drawbacks advocate for completing an emergency MRI, including 3D CE-VW imaging of extracranial arteries when GCA is suspected. With imaging, the provider could rule out GCA with higher confidence and provide a positive diagnosis faster. The early completion of MRI is paramount since MRI accuracy decreases rapidly after starting corticosteroid treatment, as soon as 3–5 days in our study which is similar to the 2–5 days reported by previous studies [8, 34, 35]. Our results are in line with recent EULAR recommendations for the management of large vessel vasculitis, mentioning that all patients presenting with signs and symptoms suggestive of GCA should be urgently referred to a specialist team for further multidisciplinary diagnostic workup and management, and that GCA should be confirmed by imaging, by using ultrasound, MRI, or both for temporal or other cranial arteries [32].

Our study suffers from several limitations. Firstly, the overall number of patients remains low. The sex-ratio is atypical in a GCA population because we would expect a threefold higher incidence of female patients. However, the prospective design of this controlled two-center study controlled against potential major bias, reinforcing the significance of our results.

Secondly, readers knew which sequences they were assessing, which could have led to a certain bias. However, they were blinded to clinical and biological data and to final diagnosis, which limits the impact of potential recognition bias.

Thirdly, we performed our study on 3-T MRI devices in two tertiary centers with optimized 2D and 3D CE-VW MR sequences, which might not be widely available across all medical centers and limit its generalization. Moreover, the MRI acquisition parameters were not the same between 2D and 3D CE-VW sequences. Our 2D acquisitions were based on the sequences already published in the literature [8, 9, 12, 14], which are currently considered sequences of reference. We designed our 3D acquisitions to take approximately the same amount of time to be conducive to clinical practice. However, the spatial resolution of the 3D sequence was lower than that of the 2D sequence, which might negatively impact analyses on small structures such as the intracranial vessel walls. Higher resolution 3D imaging might be available in the future to reduce or overcome this limitation.

Fourthly, we evaluated inter- and intra-reader variability based on a qualitative analysis instead a quantitative analysis, because the segmental and multifocal distribution of GCA made it unlikely that the readers could measure the arterial wall thickness at the same location for each extracranial artery.

Finally, we did not have pathological evidence to support our findings regarding intracranial arteries assessment; thus, we cannot be certain that all circumferential arterial wall thickenings and mural enhancements we observed were indeed GCA-related inflammatory changes, and not atherosclerotic disease. These findings should therefore be taken with caution and require further studies in which, for example, MRI follow-up of GCA patients with suspected inflammatory changes of intracranial arteries could be considered.

Conclusion

Our prospective study showed that 3D CE-VW MRI supported higher diagnostic accuracy of GCA than 2D CE-VW, with 80% sensitivity and 100% specificity. MRI should be performed as soon as possible, ideally before or within the first 5 days after corticosteroid therapy.

Acknowledgements Laura McMaster provided professional English-language medical editing of this article.

Funding information The authors state that this work has not received any funding.

Compliance with ethical standards

Guarantor: The scientific guarantor of this publication is Augustin Lecler, MD, PhD.

Conflict of interest: The authors of this manuscript declare no relationships with any companies whose products or services may be related to the subject matter of the article.

Statistics and biometry: One of the authors has significant statistical expertise.

Informed consent: Written informed consent was obtained from all subjects (patients) in this study.

Ethical approval: Institutional Review Board approval was obtained.

Methodology
- Prospective
- Diagnostic or prognostic study
- Multicenter study

References

1. Salvarani C, Cantini F, Boiardi L, Hunder GG (2002) Polymyalgiarheumatica and giant-cell arteritis. N Engl J Med 347:261–271. https://doi.org/10.1056/NEJMra011913
2. Gonzalez-Gay MA, Vazquez-Rodriguez TR, Lopez-Diaz MJ et al (2009) Epidemiology of giant cell arteritis and polymyalgia rheumatica. Arthritis Rheum 61:1454–1461. https://doi.org/10.1002/art.24459

3. Weyand CM, Hicok KC, Hunder GG, Goronzy JJ (1992) The HLA-DRB1 locus as a genetic component in giant cell arteritis. Mapping of a disease-linked sequence motif to the antigen binding site of the HLA-DR molecule. J Clin Invest 90:2355–2361. https://doi.org/10.1172/JCI116125
4. Salvarani C, Cantini F, Hunder GG (2008) Polymyalgia rheumatica and giant-cell arteritis. Lancet 372:234–245. https://doi.org/10.1016/S0140-6736(08)61077-6
5. Liozon F, Catanzano G (1982) Horton's temporal arteritis. Anatomopathologic study using light microscopy. Apropos of 123 temporal biopsies. Rev Med Interne 3:295–301
6. Lie JT (1990) Illustrated histopathologic classification criteria for selected vasculitis syndromes. American College of Rheumatology Subcommittee on Classification of Vasculitis. Arthritis Rheum 33:1074–1087
7. Vodopivec I, Rizzo JF 3rd (2018) Ophthalmic manifestations of giant cell arteritis. Rheumatology (Oxford) 57:ii63–ii72. https://doi.org/10.1093/rheumatology/kex428
8. Klink T, Geiger J, Both M et al (2014) Giant cell arteritis: diagnostic accuracy of MR imaging of superficial cranial arteries in initial diagnosis-results from a multicenter trial. Radiology 273:844–852. https://doi.org/10.1148/radiol.14140056
9. Rhéaume M, Rebello R, Pagnoux C et al (2017) High-resolution magnetic resonance imaging of scalp arteries for the diagnosis of giant cell arteritis: results of a prospective cohort study. Arthritis Rheumatol 69:161–168. https://doi.org/10.1002/art.39824
10. Bley TA, Wieben O, Vaith P, Schmidt D, Ghanem NA, Langer M (2004) Magnetic resonance imaging depicts mural inflammation of the temporal artery in giant cell arteritis. Arthritis Rheum 51:1062–1063. https://doi.org/10.1002/art.20840
11. Bley TA, Wieben O, Uhl M, Thiel J, Schmidt D, Langer M (2005) High-resolution mri in giant cell arteritis: imaging of the wall of the superficial temporal artery. AJR Am J Roentgenol 184:283–287. https://doi.org/10.2214/ajr.184.1.01840283
12. Bley TA, Uhl M, Carew J et al (2007) Diagnostic value of highresolution MR imaging in giant cell arteritis. AJNR Am J Neuroradiol 28:1722–1727. https://doi.org/10.3174/ajnr.A0638
13. Bley TA, Reinhard M, Hauenstein C et al (2008) Comparison of duplex sonography and high-resolution magnetic resonance imaging in the diagnosis of giant cell (temporal) arteritis. Arthritis Rheum 58:2574–2578. https://doi.org/10.1002/art.23699
14. Siemonsen S, Brekenfeld C, Holst B, Kaufmann-Buehler AK, Fiehler J, Bley TA (2015) 3T MRI reveals extra- and intracranial involvement in giant cell arteritis. AJNR Am J Neuroradiol 36:91–97. https://doi.org/10.3174/ajnr.A4086
15. Dejaco C, Ramiro S, Duftner C et al (2018) EULAR recommendations for the use of imaging in large vessel vasculitis in clinical practice. Ann Rheum Dis 77:636–643. https://doi.org/10.1136/annrheumdis-2017-212649
16. Bossuyt PM, Reitsma JB, Bruns DE et al (2015) STARD 2015: an updated list of essential items for reporting diagnostic accuracy studies. Radiology 277:826–832. https://doi.org/10.1148/radiol.2015151516
17. Hunder GG, Bloch DA, Michel BA et al (1990) The American College of Rheumatology 1990 criteria for the classification of giant cell arteritis. Arthritis Rheum 33:1122–1128
18. Mandell DM, Mossa-Basha M, Qiao Y et al (2017) Intracranial vessel wallMRI: principles and expert consensus recommendations of the American Society of Neuroradiology. AJNR Am J Neuroradiol 38:218–229. https://doi.org/10.3174/ajnr.A4893
19. Landis JR, Koch GG (1977) An application of hierarchical kappatype statistics in the assessment of majority agreement among multiple observers. Biometrics 33:363–374. https://doi.org/10.2307/2529786
20. R: a language and environment for statistical computing. https://www.gbif.org/tool/81287/r-a-language-and-environment-forstatistical-computing. Accessed 29 Jan 2019
21. Sommer NN, Treitl KM, Coppenrath E et al (2018) Threedimensional high-resolution black-blood magnetic resonance imaging for detection of arteritic anterior ischemic optic neuropathy in patients with giant cell arteritis. Invest Radiol 53:698–704. https://doi.org/10.1097/RLI.0000000000000500
22. Mohammed-Brahim N, Clavel G, Charbonneau F et al (2019) Three tesla 3D high-resolution vessel wall MRI of the orbit may differentiate arteritic from nonarteritic anterior ischemic optic neuropathy. Invest Radiol. https://doi.org/10.1097/RLI.0000000000000595
23. Antiga L, Wasserman BA, Steinman DA (2008) On the overestimation of early wall thickening at the carotid bulb by black blood MRI, with implications for coronary and vulnerable plaque imaging. Magn Reson Med 60:1020–1028. https://doi.org/10.1002/mrm.21758
24. Klein RG, Campbell RJ, Hunder GG, Carney JA (1976) Skip lesions in temporal arteritis. Mayo Clin Proc 51:504–510
25. Tan HW, Chen X, Maingard J et al (2018) Intracranial vessel wall imaging with magnetic resonance imaging: current techniques and applications. World Neurosurg 112:186–198. https://doi.org/10.1016/j.wneu.2018.01.083
26. Salvarani C, Giannini C, Miller DV, Hunder G (2006) Giant cell arteritis: involvement of intracranial arteries. Arthritis Rheum 55:985–989. https://doi.org/10.1002/art.22359
27. Larivière D, Sacre K, Klein I et al (2014) Extra- and intracranial cerebral vasculitis in giant cell arteritis: an observational study. Medicine (Baltimore) 93:e265. https://doi.org/10.1097/MD.0000000000000265
28. Alsolaimani RS, Bhavsar SV, Khalidi NA et al (2016) Severe intracranial involvement in giant cell arteritis: 5 cases and literature review. J Rheumatol 43:648–656. https://doi.org/10.3899/jrheum.150143
29. Lindenholz A, van der Kolk AG, Zwanenburg JJM, Hendrikse J (2018) The use and pitfalls of intracranial vessel wall imaging: how we do it. Radiology 286:12–28. https://doi.org/10.1148/radiol.2017162096
30. Matteson EL, Buttgereit F, Dejaco C, Dasgupta B (2016) Glucocorticoids for management of polymyalgia rheumatica and giant cell arteritis. Rheum Dis Clin North Am 42:75–90. https://doi.org/10.1016/j.rdc.2015.08.009
31. Quinn EM, Kearney DE, Kelly J et al (2012) Temporal artery biopsy is not required in all cases of suspected giant cell arteritis. Ann Vasc Surg 26:649–654. https://doi.org/10.1016/j.avsg.2011.10.009
32. Bowling K, Rait J, Atkinson J, Srinivas G (2017) Temporal artery biopsy in the diagnosis of giant cell arteritis: does the end justify the means? Ann Med Surg (Lond) 20:1–5. https://doi.org/10.1016/j.amsu.2017.06.020
33. Hellmich B, Agueda A, Monti S et al (2019) 2018 Update of the EULAR recommendations for the management of large vessel vasculitis. Ann Rheum Dis 215672. https://doi.org/10.1136/annrheumdis-2019-215672
34. Bley TA, Markl M, Schelp M et al (2008) Mural inflammatory hyperenhancement in MRI of giant cell (temporal) arteritis resolves under corticosteroid treatment. Rheumatology (Oxford) 47:65–67. https://doi.org/10.1093/rheumatology/kem283
35. Hauenstein C, Reinhard M, Geiger J et al (2012) Effects of early corticosteroid treatment on magnetic resonance imaging and ultrasonography findings in giant cell arteritis. Rheumatol Oxf Engl 51:1999–2003. https://doi.org/10.1093/rheumatology/kes153